Global Water Resources: Vulnerability from Climate Change and Population Growth

Charles J. Vörösmarty, *et al.*

Science **289**, 284 (2000);
DOI: 10.1126/science.289.5477.284

Science (print ISSN 0036-8075; online ISSN 1095-9203) is published weekly, except the last week in December, by the American Association for the Advancement of Science, 1200 New York Avenue NW, Washington, DC 20005.

Global Water Resources: Vulnerability from Climate Change and Population Growth

Charles J. Vörösmarty,[1,2,4,5]* Pamela Green,[1,2,4] Joseph Salisbury,[1,3,4] Richard B. Lammers[1,2,4]

The future adequacy of freshwater resources is difficult to assess, owing to a complex and rapidly changing geography of water supply and use. Numerical experiments combining climate model outputs, water budgets, and socioeconomic information along digitized river networks demonstrate that (i) a large proportion of the world's population is currently experiencing water stress and (ii) rising water demands greatly outweigh greenhouse warming in defining the state of global water systems to 2025. Consideration of direct human impacts on global water supply remains a poorly articulated but potentially important facet of the larger global change question.

Greenhouse warming continues to dominate the world's science and policy agenda on global change. One fundamental concern is the impact of this climate change on water supply (*1, 2*). The question of how human society directly influences the state of the terrestrial water cycle has received much less attention, despite the presence of the socioeconomic equivalent of the Mauna Loa curve, namely, rapid population growth and economic development. Our goal in this report is to identify the contributions of climate change, human development, and their combination to the future state of global water resources.

Assessments of water vulnerability traditionally have been cast at the country or regional scale (*2–5*). Although recent work has focused on individual drainage basins and subbasins (*1, 6, 7*), to the best of our knowledge, no global-scale study has articulated the geographic linkage of water supply to water demand defined by runoff and its passage through river networks. We present a high-resolution geography of water use and availability, analyzing the vulnerability of water resource infrastructure (*8*) to future climate change, population growth and migration, and industrial development between 1985 and 2025. We consider explicitly how the topology of river systems determines the character of sustainable water supply and its use by humans.

Mean annual surface and subsurface (shallow aquifer) runoff, accumulated as river discharge (Q), is assumed to constitute the sustainable water supply to which local human populations have access (*9*). We mapped the distribution of population with respect to relative water demand (RWD) defined as the ratio of water withdrawal or water use to discharge. We consider the domestic and industrial sectors (DI/Q), irrigated agriculture (A/Q), and their combination (DIA/Q) on a mean annual basis. Each ratio determines the degree to which humans interact with sustainable water supply and provides a local index of water stress. Values on the order of 0.2 to 0.4 indicate medium to high stress, whereas those greater than 0.4 reflect conditions of severe water limitation (*10*). We also constructed a water reuse index (ΣDIA/Q), defined as the ratio of aggregate upstream water use relative to discharge. We consider vulnerability with respect to sustainable water resources only. We make no explicit tabulation of nonsustainable supplies or withdrawals, such as the mining of groundwater, although we can draw inferences about such activities by analyzing RWD. We do not explicitly model human adaptation to climate change or development pressure, but we do incorporate estimates of future water use efficiency offered in other studies.

A recent version of the Water Balance Model (WBM) (*11*) was used to compute contemporary and future runoff at 30′ grid resolution (latitude by longitude). Runoff fields were constrained by monitoring data, and converted to discharge by integrating along digitized rivers (*12, 13*). Climate change fields were from the Canadian Climate Center general circulation model CGCM1 and Hadley Center circulation model HadCM2 used in the current Intergovernmental Panel on Climate Change (IPCC) assessment (*14*). Global means for contemporary (1961–90) runoff and river discharge were computed by the WBM using off-line atmospheric forcings from HadCM2 and CGCM1. Predictions were in substantial agreement with runoff fields based on observed discharge (*13, 15*). Results from HadCM2/WBM and CGCM1/WBM were used to predict incremental differences between contemporary and future runoff and discharge for individual grid cells. These differences were then applied to a baseline (*13*) to generate the future patterns of runoff (*16*). Mean global runoff varied in response to climate change from an increase of <1 mm year^{-1} (HadCM2/WBM) to a decrease of 17 mm year^{-1} (CGCM1/WBM) (*17*). With each runoff field, more substantial changes could be found at local and regional scales. CGCM1/WBM gave the strongest climate change signal, and we use it to exemplify key findings derived from both models.

Domestic and industrial water demand was determined by population and per capita use statistics. The geography of contemporary urban and rural population was developed from a 1-km data set (*18*). Future population distribution was determined from projections of the percent change in total, rural, and urban population from 1985 to 2025 (*19*) applied to the 1-km urban and rural population maps. Country-level water withdrawal statistics (*19*) were used to estimate contemporary water demands, but they first required standardization and spatial disaggregation (*20*). The geography of agricultural water demand was computed from irrigated land area and national use statistics (*21*). Future demands for all sectors were based on population growth, economic development, and projected changes in water use efficiency (*22*). Water withdrawals at 30′ resolution were geographically linked to digital river networks and corresponding discharge estimates.

The contemporary condition is represented by 1985, the year that is most compatible with the time span represented by the runoff climatology and historical water use statistics. Against this benchmark we formulated three scenarios to quantify the contributions of climate change and development pressure to the degree of relative water demand in 2025. The first scenario (Sc1) varied climate but fixed the magnitude and spatial distribution of human population and water withdrawals at 1985 levels. Sc2 applied projected water demands for 2025 but used runoff and discharge based on contemporary climate. Sc3 changed both climate and water demand. Total water use per capita is projected to decrease from 640 to 580 m^3 year^{-1} between 1985 and 2025. The impacts of human development under Sc2 and Sc3 will therefore generally reflect population growth and migration as opposed to intensification of water use, though results will be location specific. In relation to (*5*), our calculation of global water use in 2025 is conservative, 4700 km^3 year^{-1} compared to 5200 km^3 year^{-1}.

We compared our calculations to country-level data typically applied in global water assessments. Our national-scale aggregates of gridded DIA/Q and a recent global assessment by the United Nations (*10*) place almost the same fraction of the world's 1995 population under similar levels of water stress (Table 1). In both studies, one-third of the total population of

[1]Water Systems Analysis Group, [2]Complex Systems Research Center, [3]Ocean Processes Analytical Laboratory, [4]Institute for the Study of Earth, Oceans, and Space, [5]Earth Sciences Department, University of New Hampshire, Durham, NH 03824, USA.

*To whom correspondence should be addressed.

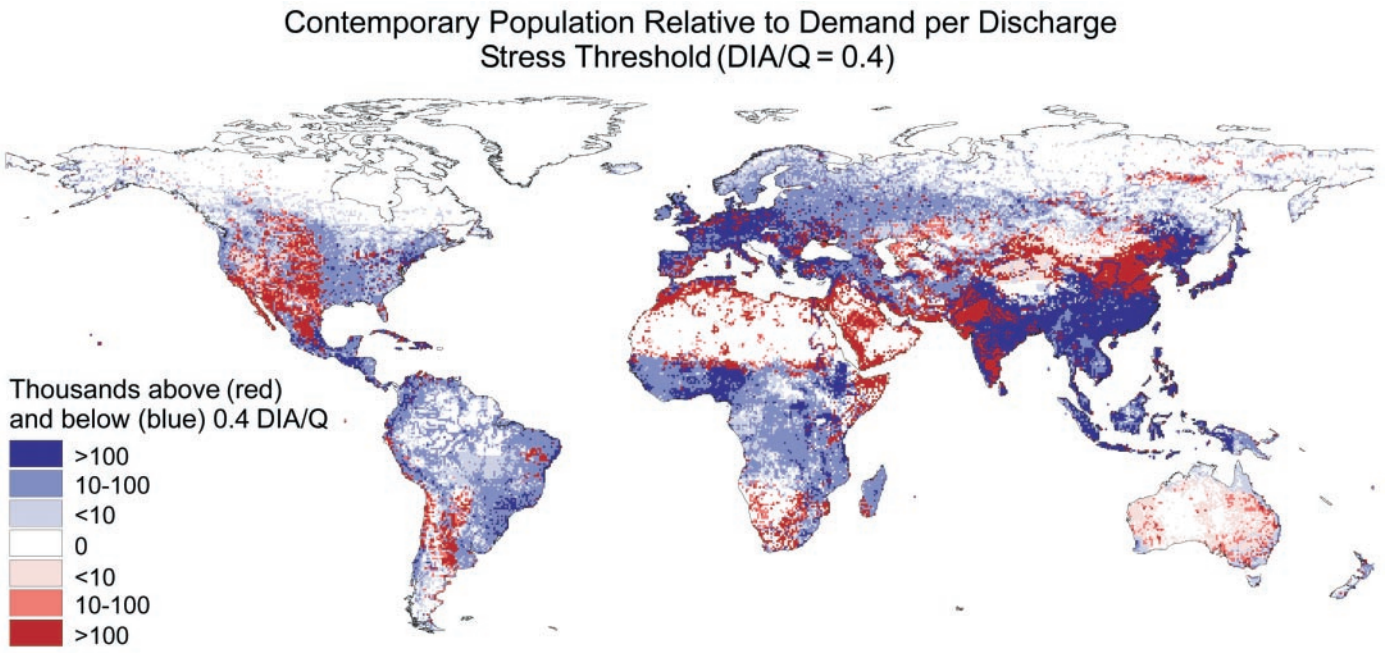

Fig. 1. The global distribution of population in 1985 with respect to the relative water stress threshold of DIA/Q = 0.4 indicating severe water scarcity (*10*). A 30′ spatial resolution is used. This mapping reflects a mean global runoff of ~40,000 km^3 year^{-1} and aggregate water withdrawals of 3100 km^3 year^{-1}. These estimates are highly dependent on contemporary water use statistics, which reflect a degree of uncertainty. Recent reviews (*5, 36*) show year 2000 global water withdrawals from assessments made even as late as 1987 to vary by >1300 km^3 year^{-1}. National-level water use statistics (*18*) for some countries are decades old. Runoff estimates for some regions may also be biased (*9,13*). Results should be viewed with appropriate caution.

Table 1. Contemporary world population living under progressive levels of relative total water demand (DIA/Q). The thresholds and definitions of water stress are as defined by the United Nations (UN) (*10*). Results shown here contrast national-level summaries (~10^2 entries) against grid-based tabulations (~10^4 to 10^5 entries). Indices given are for 1995.

Water stress	DIA/Q (unitless)	Total population (billions)		
		Country-level		Grid-based
		UN	This study*	This study
Low	<0.1	1.72	1.95	3.16
Moderate	0.1 to 0.2	2.08	1.73	0.38
Medium-high	0.2 to 0.4	1.44	1.54	0.37
High	>0.4	0.46	0.45	1.76

*Total water demand, runoff, and population at 30′ grid spatial resolution were each summed to the national scale, and corresponding aggregates were then computed.

Table 2. Cumulative distribution of worldwide population with respect to ranked values of relative water demand for domestic and industrial sectors (DI/Q) generated by the CGCM1/WBM model. Each entry represents the population at or exceeding the indicated DIA/Q level from 30′ resolution data.

DI/Q (unitless)	Cumulative population (billions)			
	Contemporary	Sc1	Sc2	Sc3
1.0	0.9	0.8	1.9	1.6
0.4	1.2	1.0	2.4	2.2
0.2	1.4	1.3	2.8	2.7
0.1	1.7	1.6	3.2	3.2
0.01	2.9	2.9	5.4	5.4
0.001	4.1	4.1	7.0	7.0
0.000	4.8	4.8	8.0	8.0

5.7 billion lives under conditions of relative water scarcity (DIA/Q > 0.2), and ~450 million people are under severe water stress (DIA/Q > 0.4). A summary based on individual grid cells (Table 1) shows that a much larger population (an additional 1.3 billion) now lives under a high degree of water stress that national-level totals, especially for large countries, fail to articulate. Use of 30′ grids (n = 59,132) captures much more of the spatial heterogeneity in water use, discharge, and RWD (Fig. 1). Water stress transcends national boundaries and is apparent today across arid and semiarid regions as well as in many densely populated parts of the humid tropics and temperate zone.

We find that the primary determinants of changing levels of RWD, and hence vulnerability to water stress, through the early part of this century will be the growth and economic development of human population. We base this conclusion on contrasts between the cumulative distributions of global population, ranked by DI/Q and A/Q, for each of the scenarios tested (Table 2). Under CGCM1/WBM, we see almost no difference between cumulative population distributions represented by the contemporary baseline and by climate change scenario Sc1. In contrast, Sc2 shows a large effect from human development with substantial increases over 1985 in accumulated population for all levels of DI/Q. The additional climatic effects represented by Sc3 fail to elicit a substantial departure from the Sc2 distribution. Although more people are predicted in 2025 to be living in relatively water-rich areas, under Sc3 the highly vulnerable population with DI/Q > 0.4 increases to >2 billion, an 85% increase in relation to the vulnerable population in 1985. This condition is determined almost exclusively by population and development pressure.

For agriculture, overall results are similar (Table 3). The population distribution here refers to the number of people dependent on irrigated water withdrawals (*21*), and changes in either remote demand or local available discharge influence A/Q under contrasting scenarios. The effect of Sc1 produces little change from 1985, and the aggregate impact of increasing water demands under Sc2 and Sc3 is apparent. For 1985, we estimate that almost 2 billion

people are dependent on irrigated lands with A/Q values of >0.4. For 2025, under Sc3 this number rises to >3 billion. Irrigation thus supports 40% of the population in 1985 (and will potentially support the same percentage in 2025) on cropland with A/Q values of >0.4, suggesting a substantial nonsustainable water use and major global vulnerability, even under present-day conditions.

Our findings are further supported by calculations expressed as continental- and global-scale totals (Table 4). For the globe, climate change under Sc1 increased DIA/Q values by <5%. In contrast, rising water demands alone (Sc2) increased DIA/Q by 50%, whereas Sc3 combining both climate and development effects produced relative increases of 60%. Over individual continents, climate-induced changes in DIA/Q varied from a 4% decrease to a 12% increase, which were in all cases much smaller than changes corresponding to population and economic growth.

Continental- and global-scale summaries mask potentially important regional patterns of water abundance and scarcity. We accumulated water demand and water supply and calculated ΣDIA/Q along main-stem rivers to establish an aggregate imprint of water use intensity and competition across watersheds. Even rivers in close proximity show distinct patterns of ΣDIA/Q and of sensitivity to future changes in climate and water demand (Fig. 2). The Chang Jiang River (China) follows a pattern of sensitivity under which both climate change and population pressures increase the water reuse index along virtually the entire main stem. Under Sc3, we see a severalfold increase in ΣDIA/Q over contemporary conditions, an impact determined in large measure by climate change. The neighboring Yellow River also displays a progressive intensification of ΣDIA/Q in the downstream direction but with an aggregate use of water well in excess of the entire basin's discharge, even for the baseline condition. Future development pressure (Sc2) exacerbates the situation, whereas climate change has an apparent beneficial effect by lowering values of ΣDIA/Q over the entire main stem, thereby counteracting the increases associated with future population growth. As a result, future ΣDIA/Q values are lowered substantially. Despite the projected improvement, there is likely to be a sustained and severe pressure on water supplies in this basin. Contemporary conditions along this river are already more severe than indicated, because of rapid increases in water use and decreases in discharge into the 1990s (*23*), which are not reflected by the 1985 benchmark.

When results are examined at the grid-cell level, an even richer set of responses emerges. The increase or decrease in ΣDIA/Q for each scenario in relation to conditions in 1985 was used to develop a geography of changing relative water demand (Fig. 3). Climate change alone (Sc1) produces a mixture of responses, both positive and negative, that is highly region

Table 3. Same as Table 2, except showing the cumulative distribution of worldwide population that is dependent on contemporary water use for irrigated agriculture at different levels of relative demand (A/Q). Dependent populations were linked to irrigation water demands within individual countries; table entries are derived from gridded 30′ data.

A/Q (unitless)	Cumulative dependent population (billions)			
	Contemporary	Sc1	Sc2	Sc3
1.0	1.5	1.4	2.7	2.7
0.4	1.9	1.8	3.4	3.3
0.2	2.2	2.1	4.0	3.9
0.1	2.6	2.5	4.7	4.7
0.01	3.8	3.8	6.7	6.6
0.001	4.5	4.5	7.6	7.6
0.000	4.8	4.8	8.0	8.0

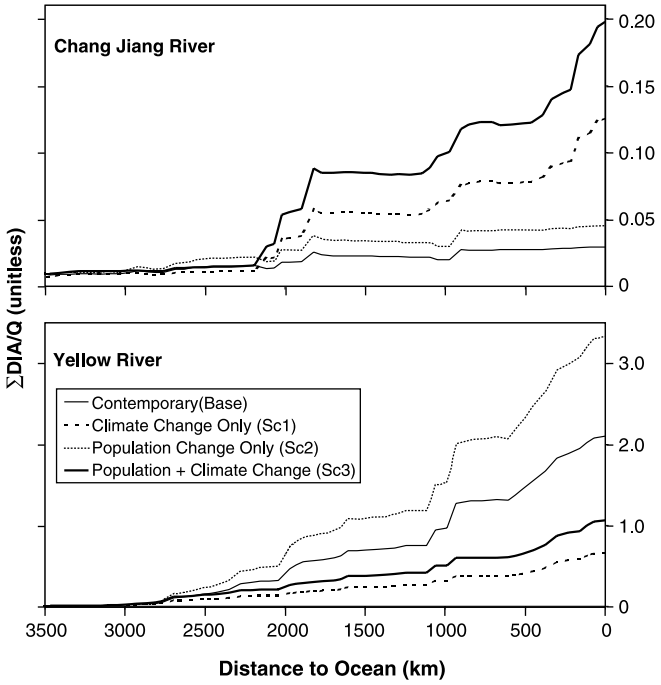

Fig. 2. The imprint of accumulated relative water demand from all sectors (ΣDIA/Q) plotted as a function of downstream distance along two major rivers in eastern Asia. The contemporary setting is contrasted against the three scenarios of potential conditions in 2025 simulated by CGCM1/WBM. Trajectories are unique for individual main-stem rivers and involve a complex interplay between the geography of river discharge and water use. An increase in this index along the downstream direction accompanies an increase in accumulated water demand, a decrease in discharge, or both, whereas a lowering of the curve reflects dilution from local runoff or less impacted tributaries. ΣDIA/Q is an index of water competition and reuse as well as a surrogate for potential water quality problems.

Table 4. Continental and global summaries for population, irrigable land, sustainable water supply defined as discharge (Q), and relative all-sector water demand (DIA/Q) tabulated for the contemporary condition and simulated by CGCM1/WBM. Percentages assigned to the change in DIA/Q (ΔDIA/Q) are relative to the 1985 contemporary baseline.

Area	Population (millions)		Irrigated cropland (1000 km²)	Observed Q (km³ year⁻¹)	Contemporary DIA/Q (unitless)	2025 Q (km³ year⁻¹)	Predicted ΔDIA/Q (%)		
	1985	2025					Sc1	Sc2	Sc3
Africa	543	1440	118	4,520	0.032	4,100	10	73	92
Asia	2930	4800	1690	13,700	0.129	13,300	2.3	60	66
Australia/Oceania	22	33	26	714	0.025	692	2.0	30	44
Europe	667	682	273	2,770	0.154	2,790	−1.9	30	31
North America	395	601	317	5,890	0.105	5,870	−4.4	23	28
South America	267	454	95	11,700	0.009	10,400	12	93	121
Globe	4830	8010	2520	39,300	0.078	37,100	4.1	50	61

specific. Expanded water use by itself (Sc2) increases relative ΣDIA/*Q* for broad regions of the globe, although small clusters of grid cells showing relative decreases appear in areas of rural-to-urban migration, as in Russia. The large continental areas with elevated ΣDIA/*Q* values under Sc3 reflect well the patterns of increase associated with Sc2. Interactions between population growth and climate change result in some notable net decreases in ΣDIA/*Q*, which are large enough to reverse the relative water scarcity suggested by Sc2, as in Mexico and much of central Asia. The overall pattern, however, is one of pandemic increase.

The major increases in relative water demand documented here reveal that much of the world will face substantial challenges to water infrastructure and associated water services. Potentially large economic costs are likely to be associated with the implementation of response strategies (e.g., expansion of facilities, new water-pricing policies, innovative technology, and mismanagement) or the consequences of inaction (e.g., deterioration of water quality and reduction in irrigated crop yields) (*24, 25*). Where sustainable water supplies are at a premium, the challenges also include curtailment of economic activities, abandonment of existing water facilities, mass migration, and conflict in international river basins (*25–27*).

Many parts of the developing world will experience large increases in relative water demand. In water-rich areas such as the wet tropics, the challenge will not be in providing adequate quantities of water, but in providing clean supplies that minimize public health problems (*28*). Arid and semiarid regions face the additional challenge of absolute water scarcity. Projected increases in scarcity will be focused on rapidly expanding cities. Much of the world's population growth over the next few decades will occur in urban areas, which are projected to double in size to near 5 billion between 1995 and 2025 (*29*) and face major challenges in coping with increased water pollution and incidence of waterborne disease (*5, 10, 19, 25, 29*).

We conclude that impending global-scale changes in population and economic development over the next 25 years will dictate the future relation between water supply and demand to a much greater degree than will changes in mean climate. To secure a more complete picture of future water vulnerabilities, it will be necessary to consider interactions among climate change and variability, land surface and groundwater hydrology, water engineering, and human systems, including societal adaptations to water scarcity [see (*30, 31*)]. Pursuit of this question will be limited by outdated and nonexistent socioeconomic data and information from a progressively deteriorating global network of hydrometric monitoring stations (*32*) unless a vigorous commitment is made by the water sciences community to collect, standardize, and widely disseminate such information. In light of our findings, an integrated approach bringing together the climate change, water resources, and socioeconomic communities appears essential to future progress.

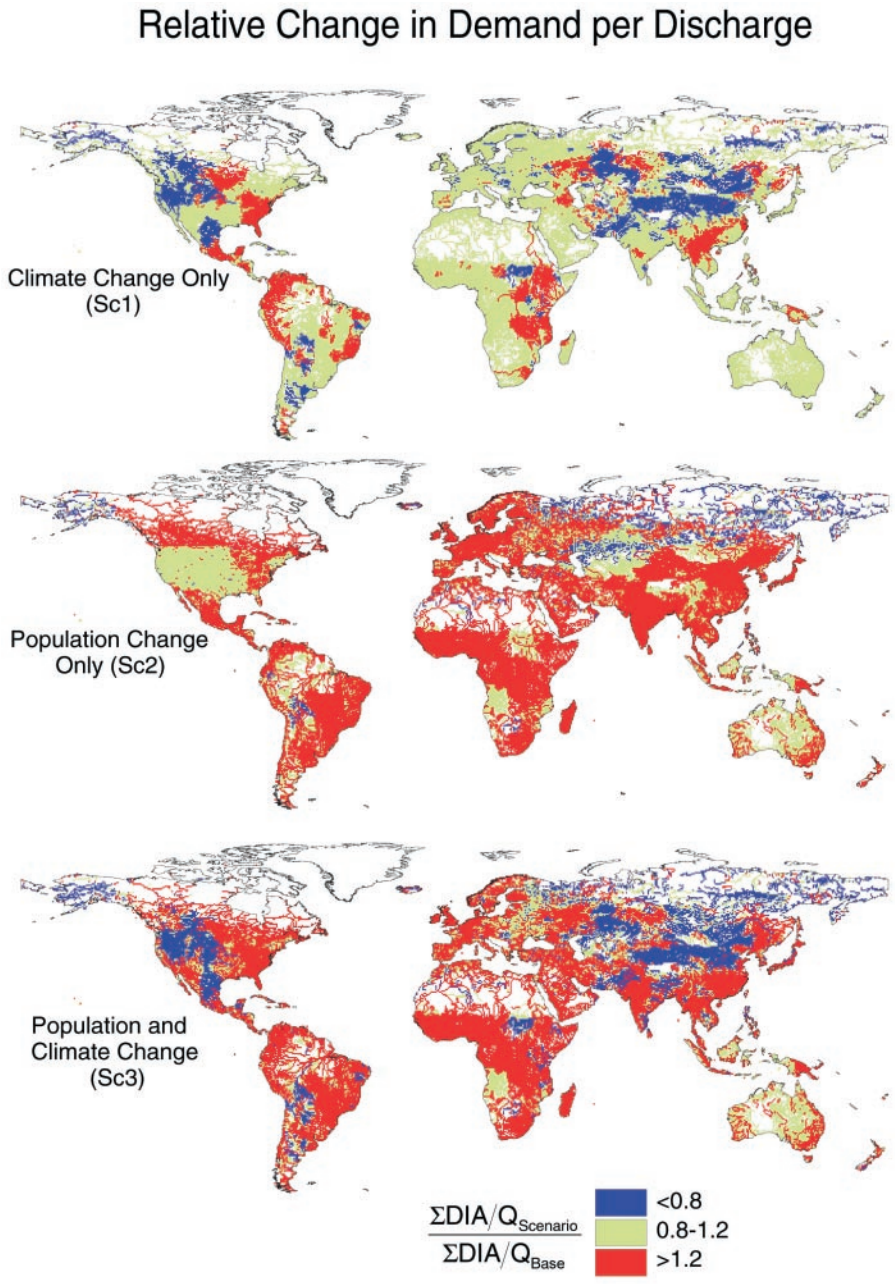

Fig. 3. Maps of the change in water reuse index (ΣDIA/*Q*) predicted by the CGCM1/WBM model configuration under Sc1 (climate change alone), Sc2 (population and economic development only), and Sc3 (both effects). Changes in the ratio of scenario-specific ΣDIA/*Q* ($\Sigma DIA/Q_{Scenario}$) relative to contemporary ($\Sigma DIA/Q_{Base}$) conditions are shown. A threshold of ±20% is used to highlight areas of substantial change.

References and Notes

1. N. Arnell *et al.*, in *Climate Change 1995: Impacts, Adaptations, and Mitigation of Climate Change*, R. T. Watson *et al.*, Eds. (Cambridge Univ. Press, Cambridge, 1996), pp. 325–363.
2. Z. Kaczmarek *et al.*, in *Climate Change 1995: Impacts, Adaptations, and Mitigation of Climate Change*, R. T. Watson *et al.*, Eds. (Cambridge Univ. Press, Cambridge, 1996), pp. 469–486.
3. M. Falkenmark, *Water Int.* **16**, 229 (1991).
4. M. I. L'vovich and G. F. White, in *The Earth as Transformed by Human Action*, B. L. Turner *et al.*, Eds. (Cambridge Univ. Press, Cambridge, 1990), pp. 235–252.
5. I. Shiklomanov, Ed., *Assessment of Water Resources and Water Availability in the World: Scientific and Technical Report* (State Hydrological Institute, St. Petersburg, Russia, 1996).
6. J. Alcamo *et al.*, in *World Water Scenarios: Analyses*, F. R. Rijsberman, Ed. (Earthscan, London, 2000), pp. 204–242.
7. J. C. van Dam, Ed., *Impacts of Climate Change and Climate Variability on Hydrological Regimes* (Cambridge Univ. Press, Cambridge, 1999).

8. "Water resource infrastructure" refers to water source, distribution, and treatment systems. We assume that wherever there is a resident human population or irrigated cropland, there will be a corresponding water infrastructure. Changes in water demand due to population growth and industrialization or in water supply due to climate change will define the vulnerability of water infrastructure and the human population that is dependent on these systems.
9. S. L. Postel *et al.*, *Science* **271**, 785 (1996).
10. United Nations, *Comprehensive Assessment of the Freshwater Resources of the World* (overview document) (World Meteorological Organization, Geneva, 1997).
11. C. J. Vörösmarty, C. A. Federer, A. Schloss, *J. Hydrol.* **207**, 147 (1998).
12. C. J. Vörösmarty, B. Fekete, M. Meybeck, R. Lammers, *Global Biogeochem. Cycles* **14**, 599 (2000).
13. B. M. Fekete *et al.*, *Global, Composite Runoff Fields Based on Observed River Discharge and Simulated Water Balances*, *Report 22* (World Meteorological Organization–Global Runoff Data Center, Koblenz, Germany, 1999).
14. Data are from the IPCC Data Distribution Centre, Deutsches Klimarechenzentrum (Max-Planck-Institut) in Hamburg, Germany, and the Climatic Research Unit at the University of East Anglia in Norwich, UK. CGCM1GSa1 and HadCM2GSa1 (GSa, ensemble of greenhouse gas plus sulfate aerosol integrations) scenarios were obtained from http://ipcc-ddc.cru.uea.ac.uk/cru_data/datadownload/download_index.html. Scenarios represent a 1% per year increase in CO_2-equivalent forcing and sulfate aerosol dampening. Original data at 3.75° by 3.75° (latitude by longitude) for CGCM1 and at 2.5° by 3.75° for HadCM2 were bilinearly interpolated to 30′ resolution. Monthly forcings were applied to the WBM, and a statistically equivalent daily time step was used to integrate over time and compute water budget variables, including runoff.
15. Simulated water budgets combined with discharge data from several hundred recording stations in (*13*) yielded a mean global runoff of 300 mm year^{-1} or a discharge of 39,300 km^3 year^{-1}; CGCM1/WBM computed respective values of 319 mm year^{-1} and 41,900 km^3 year^{-1}, whereas HadCM2/WBM gave 302 mm year^{-1} and 39,600 km^3 year^{-1}, respectively.
16. The approach taken is that used in climate impact studies on net primary production by VEMAP Members [*Global Biogeochem. Cycles* **9**, 407 (1995)].
17. The values are statistically significant ($P < 1 \times 10^{-6}$) with the Wilcoxon sign test.
18. A 1-km gridded polygon file [*Arc World Supplement*, 1:3 M scale digital map (ESRI, Redlands, CA, 1995)] defined the spatial extent of 242 countries for which country-level population statistics were available (*19*). We defined urban spatial extents as a set of geographically referenced city polygons with demographic data (n = 1858) (*33*) and distributed the remaining country-level urban population evenly across 1-km pixels classified as city lights from remote sensing (*34*). Lacking digital data to the contrary, we distributed rural population uniformly among digitized points representing populated places [*Digital Chart of the World*, 1:1 M scale digital map (ESRI, Redlands, CA, 1993)] falling outside of urban spatial extents. A total of 155 countries simultaneously showed water demand data and discharges greater than zero and fell within our 30′ digitized land mass. The remaining 87 countries were mostly small islands and were not considered. For the contemporary setting, we account for 99.7% of the global population (*19*); 98.4% of the total is assigned water use statistics.
19. *World Resources: A Guide to the Global Environment 1998–99* (World Resources Institute, Washington, DC, 1998).
20. National and sectoral water use statistics were from (*19*). The mean reporting year was 1986, but the range was from 1970 to 1995. National statistics were normalized to year 1985 by applying usage trends recorded in corresponding regional time series (*5*). Domestic water demand was computed on a per capita basis for each country and distributed geographically with respect to the 1-km total population field. Industrial usage was applied in proportion to urban population. Grid-based aggregates at 30′ resolution were then determined for domestic plus industrial water demand.
21. Country-level totals for agricultural water demand were distributed onto 30′ grid cells on the basis of the fraction of each grid cell classified as irrigated land from (*35*) and prorated on the basis of the ratio of unrealized potential evapotranspiration (i.e., the potential minus the estimated actual) to the potential from (*13*). Irrigation-dependent population was determined by proportionally assigning national-level population to the corresponding irrigated areas in each country. We reason that entire national populations (and not simply local farmers and agribusiness) benefit from the food and fiber (destined for domestic or export markets) and income produced from irrigated land. A/Q uses mean annual discharge. These relative water demand estimates are thus conservative and assume highly effective storage of surface water for irrigation, such as through reservoir impoundment. We consider irrigated agriculture because it is a major component of water resource infrastructure that is subject to changes in the availability of net runoff. Rain-fed agriculture falls outside this definition, and we have not treated it here.
22. Rates of increase in water demand to 2025 from regional estimates (*5*) were applied to the 1985 water withdrawal data set. Future changes in population and urban-to-rural ratios (*19*) were used to shift the geography of water demands. The distribution of irrigable lands was fixed to that observed under contemporary conditions. Projected water withdrawals in (*5*) are dependent on water use efficiencies that both increase and decrease for different parts of the world. These estimates were made through extensive consultation of country-level studies and trend analysis based on per unit agricultural, municipal, and industrial water withdrawals; assumptions regarding future technology adoption; and economic capacity to institute efficiency changes.
23. J. Milliman and R. Mei-e, in *Climate Change: Impact on Coastal Habitation*, D. Eisma, Ed. (CRC Press, Boca Raton, FL, 1995), pp. 57–83.
24. S. Postel, *Interciencia* **10**, 290 (1985).
25. P. Gleick, *The World's Water: The Biennial Report on Freshwater Resources (1998–99)* (Island, Washington, DC, 1998).
26. T. Homer-Dixon, *Int. Secur.* **19**, 5 (1994).
27. M. Falkenmark and J. Rockström, *Ambio* **22**, 427 (1993).
28. M. Bonell *et al.*, *Hydrology and Water Management in the Humid Tropics* (Cambridge Univ. Press, Cambridge, 1993).
29. *World Resources: A Guide to the Global Environment 1996–97* (World Resources Institute, Washington, DC, 1996).
30. D. Conway *et al.*, *Ambio* **25**, 336 (1996).
31. K. M. Strzepek *et al*, in *World Water Scenarios: Analyses*, F. R. Rijsberman, Ed. (Earthscan, London, 2000), pp. 120–159.
32. J. C. Rodda, in *Water: A Looming Crisis* (International Hydrological Program, United Nations Educational, Scientific, and Cultural Organization, Paris, 1998).
33. W. Tobler *et al.*, *The Global Demography Project*, *Technical Report TR-95-6* (National Center for Geographic Information and Analysis, Santa Barbara, CA, 1995).
34. C. Elvidge *et al.*, *Int. J. Remote Sens.* **18**, 1373 (1997).
35. P. Döll and S. Siebert, *A Digital Global Map of Irrigated Areas, Report A9901* (University of Kassel, Kassel, Germany, 1999).
36. P. Gleick, in *World Water Scenarios: Analyses*, F. R. Rijsberman, Ed. (Earthscan, London, 2000), pp. 27–37.

37. Support for this work was through the Institute for the Study of Earth, Oceans, and Space (University of New Hampshire); NASA Earth Observing System (grant NAG5-6137); NSF Division of Atmospheric Sciences (grant ATM-9707953); Office of Polar Programs (grant OPP-9524740); NASA Tropical Rainfall Monitoring Mission (grant NAG5-4785); and the U.S. Department of Energy (DE-FG02-92ER61473). We acknowledge the efforts of B. Fekete and S. Glidden in helping to develop some of the geographically referenced databases used in this study. We also thank three anonymous reviewers for their comments.

2 February 2000; accepted 3 May 2000

Overpressure and Fluid Flow in the New Jersey Continental Slope: Implications for Slope Failure and Cold Seeps

Brandon Dugan* and Peter B. Flemings

Miocene through Pleistocene sediments on the New Jersey continental slope (Ocean Drilling Program Site 1073) are undercompacted (porosity between 40 and 65%) to 640 meters below the sea floor, and this is interpreted to record fluid pressures that reach 95% of the lithostatic stress. A two-dimensional model, where rapid Pleistocene sedimentation loads permeable sandy silt of Miocene age, successfully predicts the observed pressures. The model describes how lateral pressure equilibration in permeable beds produces fluid pressures that approach the lithostatic stress where overburden is thin. This transfer of pressure may cause slope failure and drive cold seeps on passive margins around the world.

Rapid sediment loading (>1 mm year^{-1}) is documented as a source of overpressure (P^*, pressure in excess of hydrostatic) in basins around the world (*1*, *2*). A suite of models describe how overpressure is generated during rapid deposition (*3*–*6*). These models quantify the rock properties and sedimentation rates required to generate and maintain overpressure. Mass and volume measurements of wet and dry core samples provide porosity data (*7*) that we use to document overpressures on the New

503 Deike Building, Department of Geosciences, Penn State University, University Park, PA 16802, USA.

*To whom correspondence should be addressed. E-mail: dugan@geosc.psu.edu